

Theoretical study of electrolyte gate AlGa_N/Ga_N field effect transistors

M. Bayer, C. Uhl, and P. Vogl^{a)}

Walter Schottky Institute, Technical University Munich, Am Coulombwall 3, D-85748 Garching, Germany

(Received 12 August 2004; accepted 22 November 2004; published online 5 January 2005)

We predict the sensitivity of solution gate AlGa_N/Ga_N field effect transistors to *pH* values of the electrolyte and to charged adsorbates at the semiconductor–electrolyte interface. Invoking the site-binding model for the chemical reactions at the oxidic semiconductor–electrolyte interface and taking into account the large polarization fields within the nitride heterostructure, the spatial charge and potential distribution have been calculated self-consistently both in the semiconductor and the electrolyte. In addition, the source–drain current is calculated and its sensitivity to the electrolyte's *pH* value is studied systematically. Comparison with experiment shows good agreement. A significantly enhanced resolution is predicted for AlGa_N/Ga_N structures of N-face polarity. © 2005 American Institute of Physics. [DOI: 10.1063/1.1847730]

I. INTRODUCTION

Since the realization of an ion sensitive Si field effect transistor by Bergveld,^{1–3} the concept of detecting salt concentrations and charged biomolecules such as Poly-L-Lysin or DNA^{4,5} by semiconductor devices has stimulated a rapidly growing field of semiconductor-based ion sensors. Many semiconductor materials and device structures have been tested for their suitability as ion sensors. While one obtains the highest mobilities and optimal device characteristics with GaAs-based sensors,^{6–8} the toxicity of As severely hampers its physiological application. A highly promising material system that does not contain As or P is provided by a nitride semiconductor system such as Al_xGa_{1–x}N. These materials possess a chemically inert oxide surface, they are optically transparent, and extremely sensitive to changes of the surface charge or surface potential due to their high piezoelectricity and pyroelectricity that implies very large built-in electric fields.⁹ Indeed, nitride heterostructures have been shown to be competitive gas and ion detectors.^{10,11} Recently, nitride devices in contact with an electrolyte have been demonstrated to act as excellent *pH* sensors.⁹ For those structures, the reason for the dependence of the current on the *pH* value is not well understood.

In this article, we present a series of predictions and systematic theoretical studies of AlGa_N/Ga_N-based ion sensors in aqueous solutions. We consider an electrolyte on top of a Ga oxide and calculate the effect of its *pH* value and the adsorbed surface charges on the potential, charge, and current distribution inside a AlGa_N/Ga_N hetero-field-effect transistor. We calculate the two-dimensional electron gas (2DEG) density and the current parallel to the interface as a function of the surface charge density that arises from chemical reactions at the Ga oxide layer that is exposed to the electrolyte. We find the screening of this charge density by the electrolyte solution to be crucial for the understanding of the sensitivity on the *pH* value. We predict AlGa_N/Ga_N

heterostructures to act as efficient biosensors provided the 2DEG lies close to the oxide as is the case for N-face heterostructures.

In Sec. II, we briefly summarize the basic equations, such as the site-binding model and the Poisson–Boltzmann equation, that characterize the electrolyte, the chemistry of the amphoteric surface, and the charge and potential distribution within the semiconductor heterostructure. In addition, the relevant material parameters are discussed and determined by comparison with experiment. In Sec. III, we predict the *pH* sensor characteristics for Ga-face (Sec. III A) and N-face (Sec. III B) heterostructures, respectively. A brief summary in Sec. IV concludes the article.

II. THEORY

We consider a Ga_N heterostructure exposed to an electrolyte and wish to predict the change in carrier density and electric current within the semiconductor that is induced by a change in the chemical composition of the electrolyte. Specifically, the Ga_N heterostructure acts as a sensor via the semiconductor–electrolyte interface potential that reflects the adsorbed interface charges, the *pH* value, and the spatial dependence of the electric potential in the solution.

A. Model of electrolyte and amphoteric surface

In this section, we set up the theoretical model for the electrolyte and the interface reactions that we take into account. We assume the Ga_N semiconductor to be covered by a thin layer of nonstoichiometric, amorphous Ga_xO_y that forms the interface to the solution. We assume that a voltage U_G is applied across the entire semiconductor and electrolyte structure. The oxide/electrolyte interface potential and interface charge are denoted by Ψ_{ox} and $\sigma_{adsorbed}$, respectively. The latter may be positive or negative, since the oxide surface sites adsorb or desorb H⁺ ions, depending on the ionic content of the solution. In this entire discussion, we assume laterally homogeneous charge distributions so that the spatial dependencies of charges and electric potentials are effectively one-dimensional. Consequently, the charge distribution at any point within the electrolyte solution that may

^{a)}Electronic mail: vogl@wsi.tum.de

contain N types of ions is governed by the potential $\Psi(z)$ that is determined by the Poisson–Boltzmann equation,¹²

$$\epsilon_r \epsilon_0 \frac{d^2}{dz^2} \Psi(z) = \rho(z), \quad (1)$$

$$\rho(z) = -e \sum_i^N z_i n_{i,0} \exp\left\{-\frac{z_i e [\Psi(z) - U_G]}{k_B T}\right\}, \quad (2)$$

where z_i is the ion valency, e is the positive elementary charge, $n_{i,0}$ is the concentration of ion species i , and ϵ_r is the relative dielectric constant of the entire solvent. We use SI units except where specified otherwise and $k_B T$ is the thermal energy at temperature T .

In order to determine σ_{adsorbed} , we employ the so-called site-binding model for amphoteric oxide surfaces.^{1,13} This model characterizes the surface reactions by two dissociation constants K_1 and K_2 that reflect the following reactions:



Here, S denotes an oxide molecular site (Ga_xO_y in the present case) with the bonded hydroxyl group OH. These two types of reactions lead to an amphoteric behavior. When a proton gets attached to the hydroxyl group, the site gets positively charged. A dissociation, on the other hand, creates a negatively charged site. The net surface charge density is given by

$$\sigma_{\text{adsorbed}} = e(\nu_{\text{SOH}_2^+} - \nu_{\text{SO}^-}), \quad (5)$$

where $\nu_{\text{SOH}_2^+}$ and ν_{SO^-} are the charge densities of the positive and negative sites, respectively. The total number of surface groups per unit area is then given by $n_S = \nu_{\text{SOH}} + \nu_{\text{SOH}_2^+} + \nu_{\text{SO}^-}$, where ν_{SOH} denotes the density of electrically neutral sites. As shown in Healy *et al.*,¹³ the resulting dissociation constants K_1 and K_2 are given by

$$K_1 = \frac{\nu_{\text{SOH}}}{\nu_{\text{SOH}_2^+}} \exp\left[-\frac{e(\Psi_{\text{ox}} - U_G)}{k_B T} - c_{\text{pH}}\right], \quad (6)$$

$$K_2 = \frac{\nu_{\text{SO}^-}}{\nu_{\text{SOH}}} \exp\left[-\frac{e(\Psi_{\text{ox}} - U_G)}{k_B T} - c_{\text{pH}}\right], \quad (7)$$

with K_1 referring to Eq. (3) and K_2 to Eq. (4), and $c_{\text{pH}} = \text{pH} \ln 10$. We note that the pH value equals the negative decadic logarithm of the H^+ concentration, divided by M , i.e., by mole per liter. By combining expressions Eqs. (5)–(7), we finally obtain the net surface charge at the amphoteric oxide–electrolyte interface as

$$\sigma_{\text{adsorbed}} = en_S \frac{\exp(-y_0 - c_{\text{pH}}) - K_1 K_2 \exp(y_0 - c_{\text{pH}})}{K_1 + \exp(-y_0 - c_{\text{pH}}) + K_1 K_2 \exp(y_0 - c_{\text{pH}})}, \quad (8)$$

where we have introduced the abbreviation $y_0 = e(\Psi_{\text{ox}} - U_G)/k_B T$.

For the present application, we have taken into account three different types of ions, namely (i) singly charged cat-

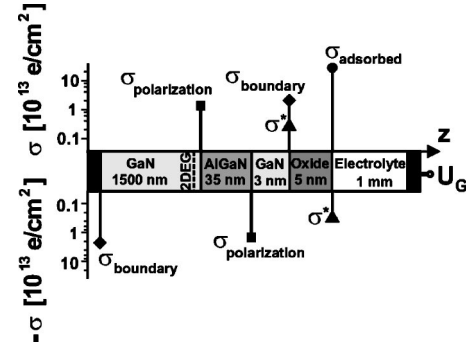


FIG. 1. Schematic layout of the calculated heterostructure including the interface charge densities. Their magnitudes, in units of 10^{13} e/cm^2 , are indicated by closed symbols and the axis to the left.

ions and (ii) singly charged anions with a fixed concentration of 100 mM that represent dissolved NaCl, (iii) a Hepes solution consisting of doubly charged cations with a concentration of 10 mM plus 20 mM singly charged anions to guarantee electrical neutrality. Any change of the pH value is compensated by a corresponding increase in the concentration of singly charged anions. Since we consider a symmetric monovalent salt and a high concentration of asymmetric divalent Hepes, a closed-form solution of the Poisson–Boltzmann equation in the electrolyte region is not possible. However, the numerical effort required to solve this equation is negligible.

B. Model of GaN heterostructure

The potential at the surface exposed to the electrolyte sets the boundary value for the potential distribution and the resulting spatial dependence of the band edge within the semiconductor device. As mentioned before, variations of the chemical features of the electrolyte, i.e., the pH value or the ionic composition, lead to detectable changes of σ_{adsorbed} and Ψ_{ox} . The relevant part in the semiconductor is the 2DEG that responds sensitively to slight changes in the spatial variation of the conduction band edge.

We consider a nitride heterostructure, grown along the hexagonal [0001] direction, that is of either Ga-face or N-face polarity. In this section, we focus on the Ga-face structure with a schematic cross section shown in Fig. 1. The structure consists of a 5-nm-thick oxide on top of a 3 nm strain-relaxed GaN layer, followed by 35 nm of an $\text{Al}_{0.28}\text{Ga}_{0.72}\text{N}$ barrier, grown on top of a $1.5 \mu\text{m}$ strain-relaxed GaN layer. The latter is assumed to be homogeneously doped with a carrier concentration of $n = 10^{16} \text{ cm}^{-3}$. This structure is a fairly typical design for GaN-based sensors that have been fabricated by several groups.^{14,15} The most significant features of AlGaIn/GaN heterostructures are the huge spontaneous and piezoelectric polarization fields. Both types of polarizations are included in our present calculations. The divergence of the total polarization across the interface between adjacent layers is equivalent to a fixed interfacial sheet charge density. There is a positive polarization charge at the left AlGaIn/GaN interface near the 2DEG in Fig. 1 with a theoretical value of $\sigma_{\text{polarization}} = 1.37 \times 10^{13} \text{ cm}^{-2}$ that is compensated at the right AlGaIn/GaN interface.^{16,17} The result-

ing polarization fields lead to a 2DEG in GaN that forms near the left interface. As we will show in Sec. III, the integrated sheet electron density $\sigma_{2\text{DEG}}$ is of the order of 10^{13} cm^{-2} . Unfortunately, only little information is available about the polarization charge at the GaN/oxide interface. It is known experimentally that no parasitic n or p channels form within the GaN layer between the barrier and the oxide layer¹⁴ for the range of σ_{adsorbed} that are considered in this article. This is consistent with a positive interface charge of $\sigma_{\text{boundary}} = 2.2 \times 10^{13} \text{ cm}^{-2}$ at the GaN/oxide interface and a compensating value at the nucleation layer (see Fig. 1). We note that the detailed value has only a small influence on the ion sensitivity of the device. By contrast, we need to take into account the following additional charge that is essential for the sensitivity. Experiments on the oxide growth on GaN have indicated voids in the oxide surface.¹⁸ Therefore some of the adsorbed ions at the oxide surface can reach the inner oxide interface by the incomplete texture of the oxide layer. We have taken into account this charge transfer by assuming that there is an additional charge $\pm\sigma^*$ at both sides of the oxide interface that amounts to some fixed percentage of the oxide/electrolyte interface charge σ_{adsorbed} . We will see in Sec. III A that the assumption of $\sigma^*/\sigma_{\text{adsorbed}} = 0.02$ is consistent with recent experiments.¹⁴ Figure 1 summarizes the structure and the position of all fixed interface charges discussed earlier in this article.

Based on these device geometries, doping densities, fixed interface charges, temperature, and Fermi–Dirac statistics, we have solved the one-dimensional nonlinear Poisson equation for the heterostructure self-consistently. The electron and hole distribution, $n(z)$ and $p(z)$, respectively, are calculated in terms of a single parabolic band model for electrons and three parabolic valence bands for holes. The electron and hole density can be written as

$$n(z) = 2 \left(\frac{2\pi k_B T m_n^*}{h^2} \right)^{3/2} F_{1/2} \left[\frac{-E_{C0,i}(z) + e\Psi(z) + E_F}{k_B T} \right], \quad (9)$$

$$p(z) = \sum_{i=1}^3 2 \left(\frac{2\pi k_B T m_{p,i}^*}{h^2} \right)^{3/2} F_{1/2} \left[\frac{E_{V0,i}(z) - e\Psi(z) - E_F}{k_B T} \right], \quad (10)$$

where $E_{C0}(z)$ is the conduction band energy, $E_{V0,i}(z)$ are the valence band energies, E_F is the Fermi energy, h is the Planck constant, $F_{1/2}[z]$ is the Fermi integral of order 1/2, m_n^* is the effective mass for the conduction band and $m_{p,i}^*$ is the effective mass for valence band number i .¹⁹ The values for the conduction and valence band energies, the band offsets of GaN and AlGaIn, as well as the strain-induced splitting and shift of the conduction and valence bands have been taken from Vurgaftman *et al.*¹⁷ The nonlinear Poisson equation has been solved on a finite-difference grid by the Newton–Raphson method; the grid size has been taken to be 0.1 nm.

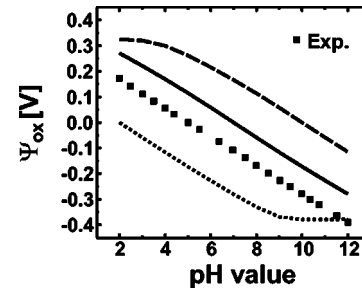


FIG. 2. Calculated oxide/electrolyte interface potential as a function of pH for an amphoteric oxide surface at zero gate voltage. The solid line depicts the result for $K_1=10^{-8}$, $K_2=10^{-6}$ and yields a sensitivity of 55.9 mV/pH. Also shown are the calculated results for $K_1=10^{-10}$, $K_2=10^{-10}$ (dashed line) and $K_1=10^{-10}$, $K_2=10^6$ (dotted line). The experimental data are from Steinhoff *et al.* (see Ref. 14).

C. Determination of material parameters

In order to perform quantitative calculations of the entire nitride/electrolyte system, we need to know the dissociation constants of the Ga_xO_y surface and the density of surface sites n_S . Recent experiments⁹ indicate that the thermal oxide Ga_xO_y on top of GaN in aqueous solution behaves similarly to Al_2O_3 . Hence, we have used the value of $n_S = 8 \times 10^{14} \text{ cm}^{-2}$ for Al_2O_3 as a starting point for Ga_xO_y .³ We have taken n_S as an adjustable parameter to reproduce the experimentally determined change in the surface potential Ψ_{ox} with the pH value of the solution.¹⁴ The results of our calculations are compared to experiment¹⁴ in Fig. 2. We note that the experimental data only determined the slope of Ψ_{ox} with the pH value, but left the absolute value undetermined. The best agreement between theory and experiment is achieved by assuming $n_S = 9 \times 10^{14} \text{ cm}^{-2}$, $K_1 = 10^{-8}$, and $K_2 = 10^{-6}$ (solid line in Fig. 2) which leads to a surface sensitivity of $\Delta\Psi_{\text{ox}}/\Delta\text{pH} = 55.9 \text{ mV/pH}$. These parameters reproduce the constant slope of $\Delta\Psi_{\text{ox}}/\Delta\text{pH}$ over the entire pH range. By contrast, dissociation constants that differ significantly from these values lead to surface potentials that saturate either for low or for high pH values. We have repeated the calculations for other values of K_1 and K_2 as specified in Fig. 2 to illustrate the dependence of Ψ_{ox} on these values.

III. RESULTS

A. Ga-face polarity

In all of the following calculations, we use the material parameters as discussed in the previous section. We can now predict the 2DEG sheet density of the GaN heterostructure with Ga-face polarity as a function of the semiconductor/electrolyte interface charge density σ_{adsorbed} , which in turn is controlled by the pH value and the gate voltage U_G . The latter has been set to zero unless stated otherwise.

The effect of an applied voltage U_G on the global potential distribution along the entire structure has been calculated by solving the Poisson–Boltzmann equation with the following boundary conditions. We have used a generalized von Neumann boundary condition at the left contact of the GaN substrate with a potential gradient that corresponds to the polarization charge $-\sigma_{\text{boundary}}$ that was detailed in Sec. II B. At the boundary of the electrolyte region to the far right in

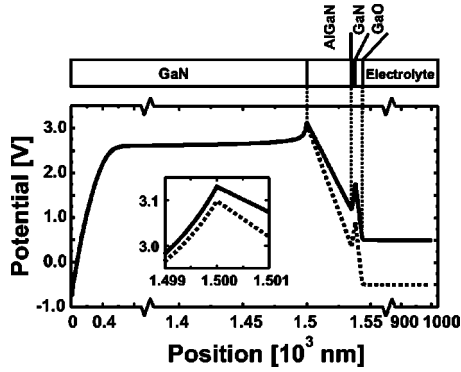


FIG. 3. Spatial potential distribution for the entire Ga-face structure with an electrolyte of $pH=5.3$. Depicted are the cases $U_G=0.5$ V (solid line) and $U_G=-0.5$ V (dotted line), respectively. The inset shows a blow-up of the potential near the position of the 2DEG.

Fig. 1, we have used a von Neumann boundary condition with zero potential gradient. We have assumed the reference potential U_G that enters Eqs. (1) and (2) to be determined by the electrode in the electrolyte solution and to be constant in the entire electrolyte region. The resulting solutions of the Poisson–Boltzmann equation are depicted in Fig. 3 for the cases of $U_G=-0.5$ and 0.5 V. Particularly the inset of this figure illustrates the effect of an externally applied bias on the potential near the 2DEG.

In Fig. 4, we show the results of our calculation of σ_{adsorbed} as a function of the pH value. As one can see, there is a range of pH values where the net surface charge density is close to zero. Nevertheless, $\sigma_{2\text{DEG}}$ does change in this region because it also depends on the surface potential Ψ_{ox} .

The present model yields a surprisingly strong dependence of the 2DEG density on the net surface charge density σ_{adsorbed} . These results are illustrated in Fig. 5. Importantly, we find that the variation of the 2DEG density with σ_{adsorbed} depends very strongly on the magnitude of σ^* . For $\sigma^*=0$ (dotted line) the relative change of the 2DEG density is noticeably smaller than for the case of $\sigma^*/\sigma_{\text{adsorbed}}=0.01$ (solid line) and $\sigma^*/\sigma_{\text{adsorbed}}=0.02$ (dashed line). As explained in Sec. II B, the physical origin of σ^* arises from either diffusion of charges through the oxide or an incomplete texture of the oxide.¹⁸ We now show that it is highly plausible to assume that the charge density σ^* at the GaN/oxide interface has a value of $\sigma^*/\sigma_{\text{adsorbed}}=0.02$. This assumption can be justified by calculating the current parallel to the interface. We have carried out the calculation of the drain current I_{SD} as a function of the source–drain–voltage U_{SD} for a HEMT

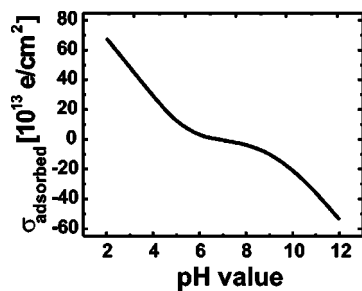


FIG. 4. Calculated variation of the oxide/electrolyte interface charge density of the amphoteric surface with the pH value.

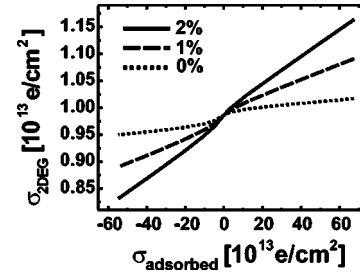


FIG. 5. Calculated results for the density of the 2DEG as a function of the surface charge density σ_{adsorbed} . The sensitivity on σ_{adsorbed} is shown for $\sigma^*/\sigma_{\text{adsorbed}}=0\%$ (dotted line), i.e., no additional sheet charge density at the GaN/oxide interface, $\sigma^*/\sigma_{\text{adsorbed}}=1\%$ (dashed line), and $\sigma^*/\sigma_{\text{adsorbed}}=2\%$ (solid line).

structure with a gate length of 1.4 μm , employing the nanodevice simulation tool²⁰ NEXTNANO³. First, we have calculated the electronic band edge energy and electron density of the system along the z axis (i.e., perpendicular to the channel) self-consistently. In the next step, we have considered a two-dimensional HEMT structure with the same sequence of layers and charge distribution as shown in Fig. 1, with a source–drain distance of 2 μm . The voltage U_{SD} has been applied across the Ohmic source and drain contacts. Figure 6 shows I_{SD} as a function of the pH value at a source–drain voltage of 0.5 mV for different fractions of $\sigma^*/\sigma_{\text{adsorbed}}$ where the source–drain current has been normalized to its value $I_{SD,0}$ at $pH=7$. The experimental data of Steinhoff *et al.*¹⁴ for a HEMT structure with the same length ratios show the same qualitative behavior of the current and are consistent with the assumed ratio of interface charges $\sigma^*/\sigma_{\text{adsorbed}}=2\%$. The data are included in Fig. 6. In the following we always used the configuration where σ^* has been taken to be 2% of σ_{adsorbed} . As one can see from Fig. 6 that the current in the semiconductor heterostructure is significantly more responsive to variations in the pH value of the electrolyte once σ^* is taken to be present. The reason is that the charge layer $+\sigma^*$ is spatially more separated from the electrolyte (see Fig. 1) and therefore gets much less efficiently screened by the ions in the aqueous solution than σ_{adsorbed} . By decreasing the oxide width, we therefore find a smaller variation in the current with the pH value in accordance with the better screening of σ^* . Similarly, this varia-

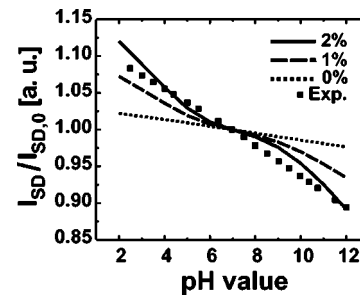


FIG. 6. Calculated dependence of the source-drain current I_{SD} on the pH value for different magnitudes of the GaN/oxide interface charge density σ^* . I_{SD} has been normalized to the source-drain current at $pH=7$ which is labeled $I_{SD,0}$. Shown are the cases $\sigma^*/\sigma_{\text{adsorbed}}=0\%$ (dotted line), $\sigma^*/\sigma_{\text{adsorbed}}=1\%$ (dashed line), and $\sigma^*/\sigma_{\text{adsorbed}}=2\%$ (solid line). The source–drain voltage U_{sd} was taken to be 0.5 mV in all cases. The experimental data are from Steinhoff *et al.* (see Ref. 14).

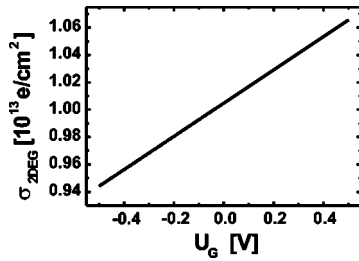


FIG. 7. 2DEG density as a function of the applied gate voltage U_G that is determined by the electrode in the electrolyte solution.

tion is reduced by decreasing the magnitude of σ^* , i.e., the fraction of σ_{adsorbed} , as shown in Fig. 6. We find these two effects to be approximately additive.

For Al contents lower than 28% in the AlGa_N layer, the density of the electrons in the 2DEG is decreased due to the smaller polarization charge density $\sigma_{\text{polarization}}$, whereas the changes of $\sigma_{2\text{DEG}}$ induced by the $p\text{H}$ value remain the same.

In Fig. 7, we depict the calculated 2DEG density as a function of the applied gate voltage where the $p\text{H}$ value has been set to $p\text{H}=5.3$. The results show that the change of $\sigma_{2\text{DEG}}$ with gate voltage U_G resembles the change that is induced by changing the $p\text{H}$ value.

B. Predictions for N-face polarity

In this section, we provide predictions on the sensitivity of nitride sensors that employ GaN heterostructures of N-face polarity. We note, however, that the chemical instability and the poorly controlled growth conditions of N-face GaN layers has hampered the successful realization of N-face AlGa_N/GaN ion sensors so far. However, their promising advantages motivate the subsequent theoretical studies. Since the conducting channel lies at the upper AlGa_N/GaN interface in this case, the carriers lie closer to the surface charge layer σ_{adsorbed} on the oxide/electrolyte interface. Consequently, the response of $\sigma_{2\text{DEG}}$ to changes in the $p\text{H}$ value as well as the applied bias is larger and provides a more efficient control of the device. We consider a structure with an increased thickness of the upper GaN layer of 15 nm. The 1500 nm GaN buffer layer has been n -doped with a concentration of $5 \times 10^{18} \text{ cm}^{-3}$ to avoid the formation of a 2DHG at the lower AlGa_N/GaN interface. The gate voltage U_G has been set to 1.2 V in order to avoid a parasitic channel in the

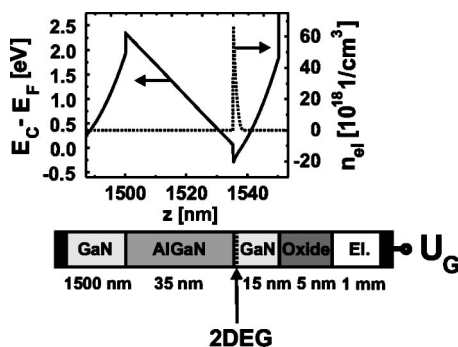


FIG. 8. Conduction band edge energy $E_C - E_F$ in eV and electron density n in 10^{18} cm^{-3} as a function of position z in nm. Also shown is the schematic cross section of the AlGa_N/GaN heterostructure of N-face polarity.

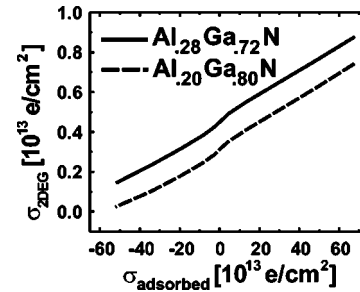


FIG. 9. Prediction of the variation of the 2DEG density with the oxide/electrolyte interface charge density σ_{adsorbed} . For an Al content of 20% (dashed line) it is possible to close the conducting channel. The solid line shows the case for an Al content of 28%.

active region. For this situation, the layout, conduction band edge $E_C(z)$, and electron density $n_{\text{el}}(z)$ are depicted in Fig. 8.

Our calculations show a significant enhancement in the variation of the 2DEG density as a function of the $p\text{H}$ value which is clearly seen in Fig. 9. The variation of the channel density $\sigma_{2\text{DEG}}$ as a function of σ_{adsorbed} is more than doubled compared to the Ga-face device.

As we pointed out in Sec. III A, a lower Al content in the AlGa_N layer improves the sensing features of the device. Indeed, when the Al fraction is reduced to 20%, the polarization charge σ_{boundary} changes from -2.2 to $-1.7 \times 10^{13} \text{ cm}^{-2}$. Since this leads to an almost vanishing value of $\sigma_{2\text{DEG}}$ for $p\text{H}$ values close to 12, the relative change in $\sigma_{2\text{DEG}}$ increases and the realization of a sensor with a closed channel at high $p\text{H}$ values is possible.

IV. SUMMARY

A model has been presented that explains the sensitivity of GaN heterostructures to surface charges that may be controlled by the $p\text{H}$ value of an electrolyte. The model for the electrolyte at an amphoteric surface is based on the solution of the Poisson–Boltzmann equation for the potential and the site-binding model for the explanation of the surface charge density on the amphoteric oxide. The 2DEG formation in the GaN heterostructure has been attributed to the large polarization fields. We have used experimental results to determine values for the dissociation constants and the concentration of sites on the oxide. The introduction of a $p\text{H}$ dependent sheet charge at the GaN/Oxide interface explains the high sensitivity of the system on the $p\text{H}$ value.

It has been further shown that N-face polarity of the GaN heterostructure will improve the sensing features significantly. Additionally, the efficiency of the sensor can be enhanced by increasing the oxide thickness as well as decreasing the Al mole fraction in the AlGa_N layer. Also, the area exposed to the electrolyte should be as large as possible relative to the total surface of the device.

ACKNOWLEDGMENTS

This work was financially supported by the Deutsche Forschungsgemeinschaft. Useful discussions with S. Birner and M. Sabathil are gratefully acknowledged.

¹P. Bergveld, IEEE Trans. Biomed. Eng. 17, 70 (1970).

- ²P. Bergveld, IEEE Trans. Biomed. Eng. **19**, 342 (1972).
- ³P. Bergveld and A. Sibbald, *Analytical and Biomedical Applications of Ion-Selective-Field-Effect-Transistors*, Analytical Chemistry Vol. XXIII, (Elsevier, New York, 1988).
- ⁴M. G. Nikolaidis, S. Rauschenbach, S. Lubner, K. Buchholz, M. Tornow, G. Abstreiter, and A. R. Bausch, Phys. Chem. Chem. Phys. **4**, 1104 (2003).
- ⁵F. Pouthas, C. Gentil, D. Côte, and U. Bockelmann, Appl. Phys. Lett. **84**, 1594 (2004).
- ⁶D. G. Wu, D. Cahen, P. Graf, R. Naaman, A. Nitzan, and D. Shvarts, Chem.-Eur. J. **7**, 1743 (2001).
- ⁷L. Chai and D. Cahen, Mater. Sci. Eng., C **19**, 339 (2002).
- ⁸S. M. Lubner, K. Adlkofer, U. Rant, A. Ulman, A. Götzhäuser, M. Grunze, D. Schuh, M. Tanaka, M. Tornow, and G. Abstreiter, Photonics Spectra **21**, 1111 (2004).
- ⁹G. Steinhoff, O. Purrucker, M. Tanaka, M. Stutzmann, and M. Eickhoff, Adv. Funct. Mater. **13**, 841 (2003).
- ¹⁰J. Schalwig, G. Müller, U. Karrer, M. Eickhoff, O. Ambacher, M. Stutzmann, L. Görgens, and G. Dollinger, Appl. Phys. Lett. **80**, 1222 (2002).
- ¹¹R. Neuberger, G. Müller, O. Ambacher, and M. Stutzmann, Phys. Status Solidi A **183**, R10 (2001).
- ¹²D. F. Evans, *The Colloidal Domain: Where Physics, Chemistry, Biology, and Technology Meet* (VCH, Weinheim, 1994).
- ¹³T. W. Healy and L. R. White, Adv. Colloid Interface Sci. **9**, 303 (1978).
- ¹⁴G. Steinhoff, M. Herrmann, W. J. Schaff, L. F. Eastman, M. Stutzmann, and M. Eickhoff, Appl. Phys. Lett. **83**, 177 (2003).
- ¹⁵C. Buchheim, A. T. Winzer, R. Goldhahn, G. Gobsch, O. Ambacher, A. Link, M. Eickhoff, and M. Stutzmann, Thin Solid Films **450**, 155 (2004).
- ¹⁶J. A. Majewski, G. Zandler, and P. Vogl, Acta Phys. Pol. A **100**, 249 (2001).
- ¹⁷I. Vurgaftman and J. R. Meyer, J. Appl. Phys. **94**, 3675 (2003).
- ¹⁸S. D. Wolter, J. M. DeLuca, S. E. Mohny, R. S. Kern, and C. P. Kuo, Thin Solid Films **371**, 153 (2000).
- ¹⁹S.-H. Wei and A. Zunger, Appl. Phys. Lett. **72**, 2011 (1998).
- ²⁰NEXTNANO³ device simulator: The program is available at www.wsi.tum.de/nextnano3 and www.nextnano.de